

Chapter 2

Spin Physics and Polarized Fusion: Where We Stand

H. Paetz gen. Schieck

Abstract A summary of the present status of nuclear fusion is given with emphasis on utilizing spin-polarized particles as fuel. The reactions considered are those concerning the four- and five-nucleon systems and especially the D + D reactions for which the status of the theory and the experimental data are presented. Recent progress has been achieved by microscopic calculations of the D + D reactions. New aspects concern e.g. the increased cross-sections at very low energies by electron screening. The need to get more experimental data is pointed out.

2.1 “Polarized” Fusion

Increasing energy demand in view of limited supply, as well as environmental and nuclear-safety concerns leading to increased emphasis on renewable energy sources such as solar or wind energy are expected to focus public and scientific interest increasingly also on fusion energy. With the decision to build ITER (low-density Magnetic Confinement Fusion, MCF) and also continuing research on (high-density) Inertial-Confinement Fusion (ICF, cf. the inauguration of the laser fusion facility at the Lawrence Livermore National Laboratory) prospects of fusion energy have probably entered a new era. The idea of “polarized fusion”, i.e. using spin-polarized particles as nuclear fuel was developed long ago ([1, 2], and for more recent developments see [3–5]).

It offers a number of modifications as compared to conventional unpolarized fusion. The main features are:

- Neutron management: replacement or reduction of neutron-producing reactions in favor of charged-particle reactions.
- Handling of the emission direction of reaction products.
- Increase of the reaction rate.

H. Paetz gen. Schieck (✉)
Institut für Kernphysik, Universität zu Köln,
Zülpicher Straße 77, 50937 Cologne, Germany
e-mail: h.schieck@t-online.de

Some of these improvements may lead to lower ignition thresholds and to more economical running conditions of a fusion reactor due to less radiation damage and activation to structures and especially the blanket, necessary to convert the neutron energy to heat, or may lead to concepts of a much simpler and longer-lasting blanket. At the same time its realization will meet additional difficulties for which solutions have to be studied. Some of these are:

- Preparation of the polarized fuel, either in the form of intense beams of polarized ^3H , D , or ^3He atoms or as pellets filled with polarized liquid or solid.
- Injection of the polarized fuel.
- Depolarization during injection or during ignition.

As an example of a recent effort to address some of these questions we cite [6–8]. The energy range in which the relevant fusion reactions will take place is <100 keV where the Coulomb barrier strongly suppresses charged-particle cross-sections. This is the reason why necessary experimental polarization data with sufficiently high precision such as spin-correlated cross-sections have not been measured. Existing reaction analyses and predictions for polarized fusion relied on existing world data sets of other (simpler) data. On the other hand, sufficiently microscopic and therefore realistic theoretical predictions (such as for the three-nucleon system) are just beginning to become available for the four-nucleon systems at the required low energies [9, 10]. An interesting question is whether the recently discussed electron-screening enhancement ([11] and references therein) of the very-low energy cross-sections has any bearing on polarized fusion.

It should be mentioned here that in the past polarization observables played a decisive role in elucidating the reaction mechanisms of few-body reactions as well as the nuclear structure of few-body nuclei, especially in the two- to six-body systems. At present only four- or five-nucleon systems are considered for fusion energy.

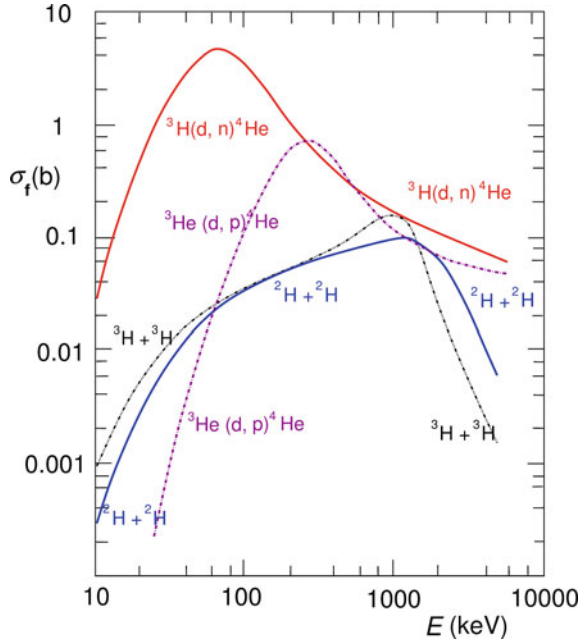
2.1.1 Fusion Basics

Here a few quantities relevant for fusion (as well as for nuclear astrophysics) at low energies will be recapitulated. These are the basic cross-sections, the reaction parameter which determines the reaction rates in a thermonuclear reactor, and the power density which depends also on the reaction-particle densities.

2.1.2 Nuclear Cross-Sections

The known low-energy reactions between charged particles that are of interest for fusion energy encompass a relatively large number of fusion reactions. Because at low energies the cross-sections are determined by the Coulomb barrier and thus—depending on the nuclear charge—are very low, in the near future only four to

Fig. 2.1 Integrated cross-sections of fusion reactions as functions of the energy of relative motion



six-nucleon systems are of interest. The basic cross-sections of the relevant nuclear low-energy reactions are shown in Fig. 2.1. The resonant behavior of the five-nucleon reactions is clearly visible whereas other reactions such as the D + D reactions appear non-resonant. It is also evident how the cross-section towards lower energies is entirely dominated by the Coulomb penetrability.

Other systems are e.g. $d+{}^6\text{Li}$ with several outgoing channels and the $p+{}^{11}\text{B}$ systems with the latter having only charged-particles in the outgoing channel.

In order to separate the influence of the Coulomb penetrability from the nuclear-reaction part it is customary to introduce the astrophysical S -factor $S(E)$ which is defined, using the Sommerfeld parameter with Z_1, Z_2 the charge numbers, and μ the reduced mass of the entrance-channel particles

$$\eta_S = \frac{Z_1 Z_2 e^2}{\hbar v} = Z_1 Z_2 \left(\frac{e^2}{\hbar c} \right) \frac{c}{v} = Z_1 Z_2 \frac{\alpha}{\beta} = \sqrt{\frac{\mu}{2E_{c.m.}}} \frac{Z_1 Z_2 e^2}{\hbar}. \quad (2.1)$$

For S waves only and assuming a point-Coulomb interaction of the bare nuclei it is

$$S(E_{c.m.}) = \sigma_{\text{tot}}(E_{c.m.}) E_{c.m.} e^{2\pi\eta_S}. \quad (2.2)$$

For purely S-wave, non-resonant, reactions in a limited range of low energies such as the D + D reactions the S -factor is smooth and practically energy-independent, higher partial waves cause an increase, and resonances show the typical excursions.

At the very low end of the energy scale the effects of screening, see Sect. 2.5.2, of the Coulomb potential by the presence of electrons (either in the plasma of gaseous reaction partners or in the metallic environment of solid target materials) will modify (increase) the fusion cross-sections appreciably, see e.g. [12]. The present status of experiments and theory is e.g. also given in [11]. The quantities relevant for fusion-energy studies thus are the integrated (or total) cross-section σ and, derived from this, the S -factor, the reaction coefficient (or reaction parameter) $\langle\sigma v\rangle$, and the (relative) power density P_f . The reactions via the five-nucleon system have the highest cross-sections and have therefore the highest priority in the research of fusion power applications with the maximum cross-section of the ${}^3\text{H}(d, n){}^4\text{He}$ reaction occurring at the lower energy.

2.2 Five-Nucleon Fusion Reactions

The important reactions to be discussed here are

- $d + {}^3\text{H} \rightarrow n + {}^4\text{He} + 17.58 \text{ MeV}$,
- $d + {}^3\text{He} \rightarrow p + {}^4\text{He} + 18.34 \text{ MeV}$.

The two mirror reactions have some very pronounced features: At the low energies discussed here both proceed via strong S-wave resonances (at deuteron laboratory energies of 107 keV for ${}^3\text{H}(d, n){}^4\text{He}$, and 430 keV for ${}^3\text{He}(d, p){}^4\text{He}$, respectively). These resonant states are quite pure $J^\pi = 3/2^+$ states with possibly very little admixture of a $J^\pi = 1/2^+$ S-wave and/or higher-wave contributions. This has been a long-time point of discussion, mainly because of the reactions being very good absolute tensor-polarization analyzers, provided they proceed only through the S-wave, $J^\pi = 3/2^+$ state. Experimental evidence shows that other contributions are small (on the order of a few %). An example of the ${}^3\text{He}(d, p){}^4\text{He}$ reaction on resonance is an early spin-correlation measurement [13, 14] supporting this assumption, see Fig. 2.2. For a recent discussion of this reaction at low energies see e.g. [15, 16]. The results for the mirror reaction ${}^3\text{H}(d, n){}^4\text{He}$ are similar.

The relatively good knowledge about these two reactions allows the conclusion that with polarized beams and targets an enhancement of the fusion yield close to a factor of 1.5 may be expected. A simple hand-waving statistical argument shows that the reactions, if they go entirely through the $3/2^+$ state and with the entrance channel prepared in a stretched configuration, as compared to the unpolarized entrance channel with a purely statistical spin configuration, yield just this enhancement. Earlier analyses of existing data (see e.g. [17, 18]) had to use simplifying assumptions such as linear relations between data while neglecting small square terms. Only if improvements in our present quantitative knowledge about the $A = 5$ reaction details are desired would the very tedious and difficult experiments seem necessary.

Another interesting feature of polarizing the fuel for the two five-nucleon reactions is the possibility of controlling the emission directions of the neutrons (protons) and also the α particles. The angular distributions for unpolarized nuclei at the

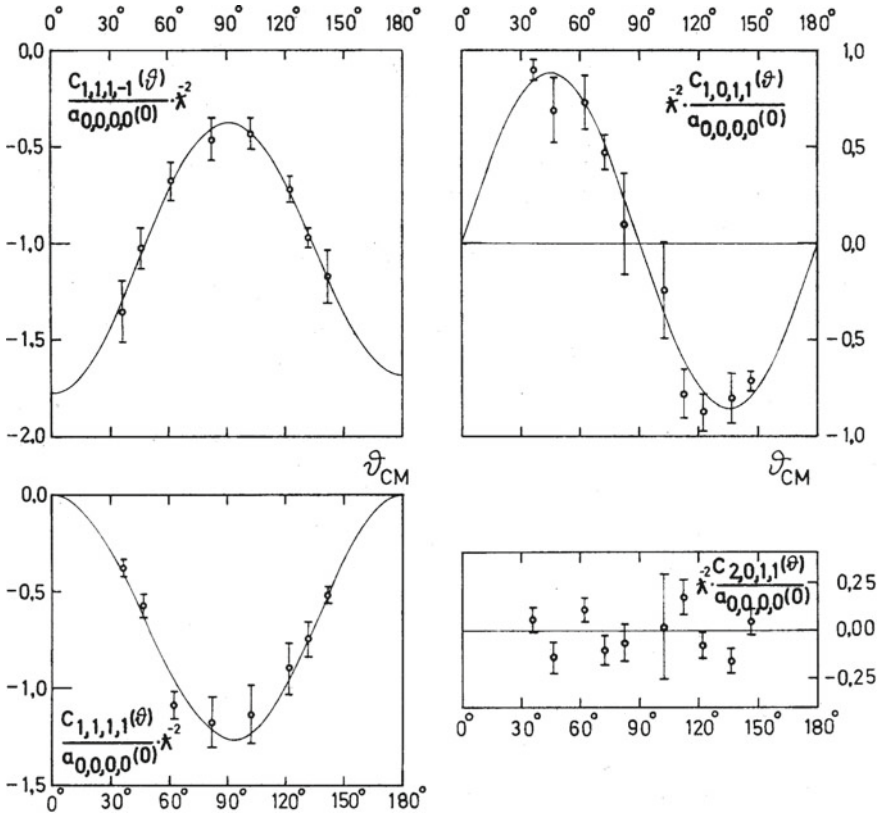


Fig. 2.2 Spin-correlation measurement of the ${}^3\text{He}(\vec{d}, p){}^4\text{He}$ reaction at $E_{d,lab} = 430$ keV. This energy corresponds to that of the S-wave $J^\pi = 3/2^+$ resonance. The lines are least-squares Legendre fits. From [13]. By permission of Schweizerische Physikalische Gesellschaft SPG, Basel

resonance energies are isotropic in the c.m. system (with pure S wave assumed) resulting in a small anisotropy in the laboratory system. The angular anisotropies of the tensor analyzing power $A_{zz}(\theta)$ and also of $C_{z,z}(\theta)$, the spin-correlation coefficient with all nuclei vector-polarized along the magnetic field (e.g. of a tokamak reactor), follow a $P_2(\cos \theta)$ distribution. These anisotropies determine the cross-section angular distributions, see the Appendix. Figure 2.3 shows the anisotropies due to polarization and kinematics of a few spin observables and cross-sections. Using these anisotropies neutrons could be diverted away from the walls and alpha particles directed into the plasma enhancing the plasma temperature. For a realistic representation of the anisotropies in a thermal plasma these (nuclear) anisotropies in the laboratory system must be folded with the Maxwell-Boltzmann energy (velocity) distribution over the region of the Gamow peak (as has been done by Hale and Doolen

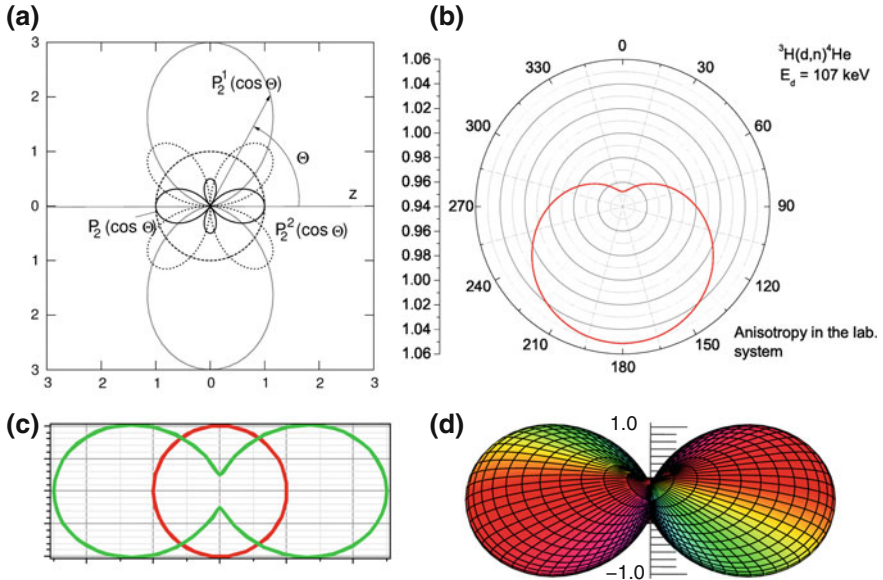


Fig. 2.3 **a** Typical anisotropies of observables for S-wave spin-1 on spin-1/2 reactions: The anisotropy $\propto P_2(\cos \theta)$ of the tensor analyzing power $A_{zz}(\theta)$ and the longitudinal vector–vector spin correlation coefficient $C_{z,z}(\theta)$, as well as that of the tensor–vector spin correlation coefficients $C_{zz,y}(\theta) \propto P_2^1(\cos \theta)$, and the transverse vector–vector coefficient $C_{y,y}(\theta) \propto P_2^2(\cos \theta)$ of the reactions ${}^3\text{H}(d, n){}^4\text{He}$ or ${}^3\text{He}(d, p){}^4\text{He}$ are displayed. **b** Kinematical anisotropy in the laboratory system of the isotropic c.m. cross-section. **c** “Polarized” cross-section anisotropy compared to the unpolarized case (*red circle*). **d** Anisotropy in the simplest case of the “polarized” longitudinal correlation cross-section $d\sigma_{pol}/d\sigma_0 = 1 + \frac{3}{2}p_z q_z C_{z,z}(\theta)$ of a reaction between vector-polarized spin-1 and vector-polarized spin-1/2 particles (both aligned in the z direction and with $p_z = q_z = 1$). The analyzing power $A_z(\theta)$ and the tensor–vector correlation coefficient $C_{zz,z}(\theta)$ are parity-forbidden

for the $\text{D} + \text{D}$ reactions [4, 19]), but for the 5-nucleon reactions at low energies the effects are expected to be small.

It has also been argued [20] that for a tokamak near ignition the ignition conditions change non-linearly with the reactivity thus leading to increases of gains by more than 50 % using polarized fuel. For both mirror reactions small admixtures, especially from the S wave $1/2^+$ and from higher-wave states cannot be excluded. A total of 13 matrix elements with up to $L = 2$ is possible, see e.g. [17]. The available data do not suffice to determine their (small) contributions unambiguously. Only the $1/2^+$ state is estimated to contribute less than 5 % on resonance. Much below the resonance it may contribute substantially more but the unpolarized cross-sections will just have another isotropic (in the c.m. system) contribution that could only be disentangled in a complete matrix-element analysis. From the total number of possible polarization observables only the S-wave case with polarizations along the z direction (three examples) will be discussed here.

- The unpolarized cross section is

$$\left(\frac{d\sigma}{d\Omega}\right)_0 = \frac{\lambda^2}{6} \left(|T_{3/2^+}|^2 + \frac{1}{2}|T_{1/2^+}|^2 \right). \quad (2.3)$$

- No vector, but tensor analyzing powers and spin correlations $\neq 0$ can occur, see the Appendix.
- The cross-section for incident S-wave deuterons with tensor polarization p_{zz} on an unpolarized ${}^3\text{H}$ target contains $T_{1/2^+}$ only in an interference term between the two matrix elements, i.e. $T_{1/2^+}$ enters linearly in contrast to the unpolarized cross-section

$$\left(\frac{d\sigma}{d\Omega}\right)_{pol} = \left(\frac{d\sigma}{d\Omega}\right)_0 + \frac{\lambda^2}{6} \left(-\frac{1}{2}\right) \left[|T_{3/2^+}|^2 + 2\Re(T_{3/2^+} T_{1/2^+}^*) \right] P_2(\cos \Theta) p_{zz}. \quad (2.4)$$

- The pure vector–vector “aligned” spin-correlation cross-section contains an isotropic term, adding to the unpolarized angular distribution, and another $P_2(\cos \Theta)$ term:

$$\left(\frac{d\sigma}{d\Omega}\right)_{pol} = \left(\frac{d\sigma}{d\Omega}\right)_0 + \frac{\lambda^2}{6} \left\{ -\Re(T_{3/2^+} T_{1/2^+}^*) + \left[-|T_{3/2^+}|^2 + \Re(T_{3/2^+} T_{1/2^+}^*) \right] P_2(\cos \Theta) p_z q_z \right\}. \quad (2.5)$$

2.3 Four-Nucleon Reactions

The most important four-nucleon fusion reactions are the D + D reactions which, in a plasma, also inevitably accompany the more important five-nucleon reactions discussed above

- $d + d \rightarrow n + {}^3\text{He} + 3.268 \text{ MeV}$,
- $d + d \rightarrow p + {}^3\text{H} + 4.033 \text{ MeV}$.

Whereas the situation of the five-nucleon systems is relatively clear-cut the four-nucleon systems and especially the two D + D reactions have a number of problems in their description, especially in view of “polarized fusion”. Different from the five-nucleon case the non-resonant reaction mechanism is very complicated (at least 16 complex matrix elements including S, P, and D waves have to be considered with spin-flip transitions from the entrance to the exit channel which contribute even at low energies). One consequence of participating P waves is that they are the only reactions with appreciable vector- (besides tensor-)analyzing power even down to 20 keV laboratory energy which makes them very useful analyzer reactions at these energies (see also [4, 5]). In a semi-classical picture this is made plausible with the large extension of the deuteron wave function and therefore large interaction distance of the two deuterons.

2.3.1 *Suppression of Unwanted D + D Neutrons*

Aneutronic fusion may have a number of advantages (not the least unimportant *economic* ones) over the use of neutron-producing reactions. At an advanced stage the ${}^3\text{H}(\text{d}, \text{n})$ reaction could be replaced by the ${}^3\text{H}(\text{d}, \text{p})$ reaction. However, D + D neutrons would remain. It has been suggested by theoretical approaches that D + D neutrons could be reduced substantially by polarizing the deuterons, thus forming a quintet ($S = 2$) state. The main argument was that quintet states in the entrance channel would require spin-flip transitions which are Pauli-forbidden in first order. However, this argument would be invalid if the reactions proceeded via the D state of the deuteron, and so far the (indirect) experimental evidence does not support this conjecture, see e.g. [4]. For all of these reasons the prediction of suppression or enhancement of the D + D reactions is not possible by considering spin coupling only but requires detailed theoretical and experimental studies. All more recent and more modern studies point to relatively small, if not zero suppression or even some enhancement below 100 keV. A direct spin-correlated cross-section measurement is still lacking, but is highly desirable.

2.3.1.1 Evidence for Suppression?

Lacking a direct spin-correlation experiment at very low energies, several indirect approaches have been taken, two of which are:

1. Parametrization of world data by a multi-channel R-matrix analysis [21].
2. Köln parametrization of world data of the ${}^2\text{H}(\text{d}, \text{n}){}^3\text{He}$ and ${}^2\text{H}(\text{d}, \text{p}){}^3\text{H}$ reactions by direct T-matrix analysis below 1.5 MeV including S, P, and D waves (16 complex matrix elements) [22–24].

Both approaches allow predictions of any observable of the D + D reactions, also of the *Quintet Suppression Factor QSF* and similar suppression factors for other spin configurations, as defined below. The parametrization 2 is the least model-dependent and will be discussed here in some detail.

2.3.2 *Formalism and Theory of the D + D Reactions*

The assumption that the total cross-section is governed by the Coulomb barrier at low energies leads to a model in which the nuclear matrix elements are assumed constant and the energy dependence is that of the L -dependent and calculable Coulomb penetrabilities which can be factored out. However, the calculation of the latter requires a (weak) model assumption too. Whereas for a point nucleus the calculation is straightforward, for an extended nucleus the definition of the penetrability depends on the interaction distance r_0 and assumptions on the interaction where usually *hard-sphere scattering* is assumed [25, 26] (for the discussion of other models see

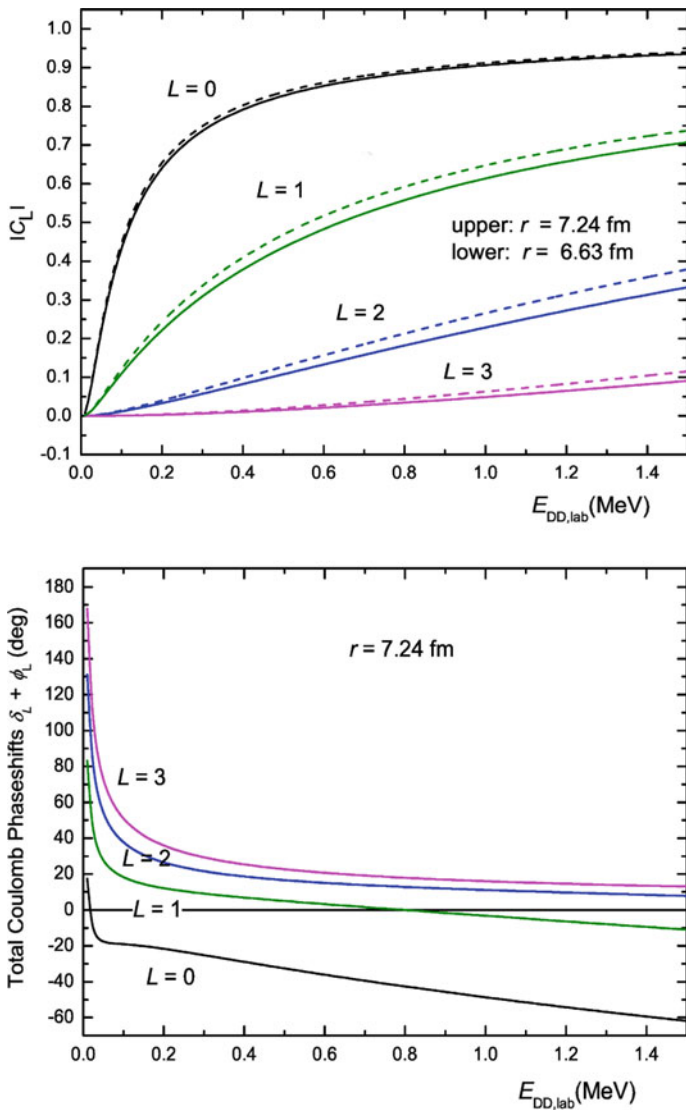


Fig. 2.4 Coulomb transmission factors and total phase shifts as functions of the lab energy of the D + D reactions. Hard-sphere behavior of the reaction has been assumed

e.g. [27]). The total phases are then a sum over those for point nucleus scattering and the hard-sphere phases. Figure 2.4 shows the transmission factors $|C_L|$ and the phases as functions of the incident energy. F_L and G_L are the regular and irregular Coulomb wave functions. The definitions are (with $\rho = kr_0$ and η the Sommerfeld parameter):

$$\text{the complex transmission } C_L = \sqrt{P_L(\rho)} \exp^{i(\delta_L + \phi_L)}, \quad (2.6)$$

$$\text{the hard-sphere phases } \delta_L = \tan^{-1} \frac{F_L(\rho)}{G_L(\rho)}, \quad (2.7)$$

$$\text{and the Coulomb scattering phases } \phi_l = \arg \Gamma(L + 1 + i\eta). \quad (2.8)$$

The model assumptions are expressed by the factor g :

$$|C_L| = \left(\frac{g}{F_L^2 + G_L^2} \right)^{1/2} \quad \text{with } g = \begin{cases} 1 & \text{(point nucleus),} \\ F_L^2 & \text{(hard sphere),} \\ kr_0 & \text{(black nucleus).} \end{cases} \quad (2.9)$$

The transition matrix consists of constant ‘‘internal’’ matrix elements multiplied with the energy-dependent transmission factors

$$\mathbf{T}_{\beta\alpha}(E) = C_L(E, r_0) \times \tilde{\mathbf{T}}_{\beta\alpha}. \quad (2.10)$$

In a least-squares fit procedure the best-fit matrix elements were determined using Legendre coefficient expansions of all available D + D data. The dependence on r_0 is weak, and the transmission factors are small except for $L = 0$. With this ansatz a determination of all 16 transition matrix elements for both D + D reactions at low energies was possible (see [22, 23] for the neutron and proton channels up to 500 keV and [24] for the proton channel up to 1500 keV). Using these matrix elements all observables of both reactions can be predicted, especially also the influence of the polarization of the fuel nuclei on the fusion process.

The results of this analysis have been discussed in detail in [4] with many figures and references.¹

Since these analyses the D + D data base has not experienced much improvement by new data. New unpolarized (however not absolutely calibrated) differential cross-section data for both reactions [28] and two polarization-transfer measurements for ${}^2\text{H}(d, p){}^3\text{H}$ [29, 30] in the energy range discussed here should be cited. However, it is not expected that these additional data would substantially change the predictions summarized in Fig. 2.5.

2.3.2.1 Definition of the Quintet Suppression Factor

In order to quantify the extent to which D + D neutrons may be suppressed by polarizing the fusion fuel nuclei the *Quintet Suppression Factor QSF* has been defined.

$$QSF = \frac{\sigma_{1,1}}{\sigma_0}, \quad (2.11)$$

¹The Fig. 19 of that reference was meant to compare the proton versus neutron channel and the data is from an early fit and not calibrated. The ordinate scale should be understood as arbitrary and the result for the proton channel is correctly given in Fig. 23.

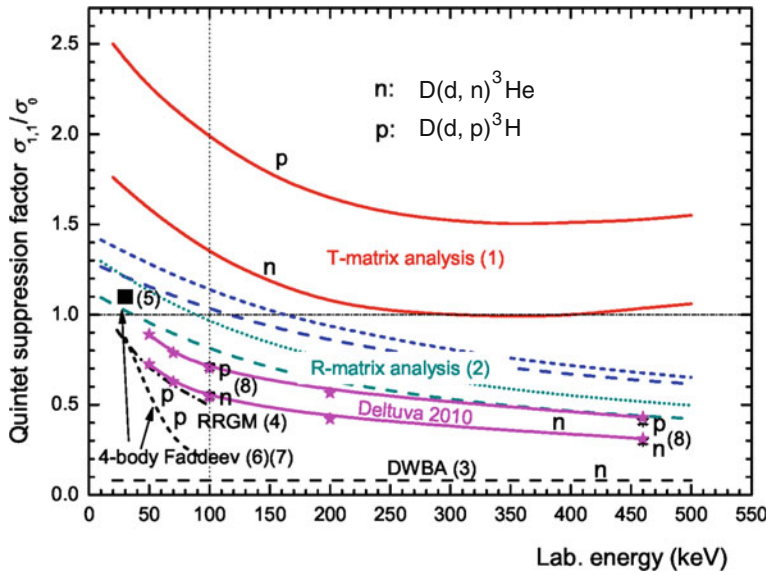


Fig. 2.5 Quintet suppression factor as predicted by various theoretical and from two experimental approaches using the world data of the D + D reactions. The relevant references (numbers in parentheses in the figure) are: (1): [23] (*thick solid lines*), (2): [19, 31], (3): [32, 33], (4): [34–36], (5): [37], (6): [38], (7): [39], and (8): [9, 10] (*stars and thin solid lines*). The predictions of [9, 10, 37, 38] are from microscopic Faddeev–Yakubovsky calculations

where

$$\sigma_0 = \frac{1}{9} \left(\underbrace{2\sigma_{1,1}}_{\text{Quintet}} + \underbrace{4\sigma_{1,0}}_{\text{Triplet}} + \underbrace{\sigma_{0,0} + 2\sigma_{1,-1}}_{\text{Singlet}} \right) \quad (2.12)$$

is the total (integrated) cross-section to which the four independent channel-spin cross-sections $\sigma_{1,1}$ (spin-quintet configuration), $\sigma_{1,0}$ (spin triplet), $\sigma_{0,0}$, and $\sigma_{1,-1}$ (two spin-singlet terms) contribute with their statistical weights.

In Fig. 2.5 all results for the QSF from different theoretical predictions as well as from the two data parameterizations for both D + D reactions are shown. The theoretical approaches reach from DWBA calculations to very recent microscopic calculations including the Coulomb force [9, 10] and vary widely. However, these latest and most advanced calculations lend confidence to the idea that substantial suppression occurs only in the higher energy range, i. e. above the region of the Gamow peak at which fusion-energy production will preferably take place.

2.3.3 Possible Reaction-Rate Enhancement for the $D + D$ Reactions by Polarization?

Whereas the appreciable enhancement of the reaction rate for the two principal five-nucleon reactions can be considered certain this effect has to be investigated for the two $D + D$ fusion reactions.

Although these reactions will not be first choice for a fusion reactor, needing higher temperatures, they should be considered for more developed concepts. They would not need either ^3H or ^3He , both of which would have to be “bred” artificially in contrast to ^2H which may be extracted from seawater in sufficient quantities. The lower energies of the ejectiles of these reactions (neutrons and protons) may also have advantages or disadvantages compared to those of the ^3H and ^3He reactions.

Because the $D + D$ reactions inevitably accompany the main fusion reactions a possible rate enhancement (or attenuation) has to be weighed against a possible rate suppression (or enhancement) by polarizing the fuel.

2.4 Present Status of “Polarized” Fusion

In view of the wide range of theoretical predictions and the lack of direct experimental evidence e.g. for the QSF it seems mandatory to perform a direct $D + D$ spin-correlation experiment in the energy range from 10 to 100 keV. The number of correlation coefficients, however, is quite formidable, see the Appendix and [4, 5].

The simplest correlation experiment is that with both deuterons polarized in the z (the beam) direction

$$\left(\frac{d\sigma(\Theta, \phi)}{d\Omega}\right)_{\phi=0} = \left(\frac{d\sigma(\Theta)}{d\Omega}\right)_0 [1 + C_{z,z}(\Theta)p_zq_z + C_{zz,zz}(\Theta)p_{zz}q_{zz}]. \quad (2.13)$$

Simplifications in the general formalism are achieved by selection of polarization components along single coordinates and the choice of pure vector or tensor polarizations at the beam source (correlation terms such as $C_{z,zz}$, $C_{zz,z}$, $C_{xz,x}$, $C_{yz,y}$, or $C_{yz,zz}$ as well as the analyzing powers $A_z(b)$, $A_x(b)$, $A_z(t)$, or $A_x(t)$ are forbidden under parity conservation).

The main difficulties with spin-correlation measurements at these low energies are:

- the low cross-sections.
- The use of solid polarized targets can be excluded because it appears impossible to make them sufficiently thin. Therefore only two interacting polarized beams may be employed resulting in low target densities and small yields.
- The use of (compressed) polarized gas at these low energies meets the difficulties of the need for a container including very thin and, at the same time, strong windows of polarization-conserving materials.

Thus, the only sensible experimental arrangement for measuring spin correlations for the $D + D$ reactions is using an intense atomic beam of polarized deuterons as target which is crossed by another atomic or ion beam of polarized deuterons.

Alternatively, one could think of building a low-energy storage-ring device in analogy to COSY-Jülich where multiple target passes would compensate for the low cross-sections. However, the technical and financial requirements on such a device seem prohibitive. The high forward multiple-scattering cross-section e.g. would require extremely good vacuum.

2.5 New Calculations for Few-Body Systems

A phenomenon studied only rather recently is the enhancement of cross-sections of few-nucleon reactions at the very-low-energy range. Although for fusion-energy production this may be a favorable feature, for nuclear astrophysics of the Big-Bang scenario this constitutes a problem because the extrapolation of the S -factor to even lower energy ranges than measured is uncertain as long as there is no reliable theoretical guideline helping to extract the bare nuclear cross-sections needed for astrophysics. Therefore, exact predictions of the pure nuclear cross-sections from microscopic theories are urgently needed.

2.5.1 Theoretical Approaches

So far—following the progress in theoretical descriptions of the three-nucleon systems—predictions for the four-nucleon systems have been based on resonating-group and Faddeev–Yakubovsky calculations. The high-accuracy nucleon–nucleon interaction data have been used as input. Recent improvements have been achieved by including the Coulomb interaction in a satisfactory way [9, 10] and by using the effective-field theoretical approach. One quantity of interest for polarized fusion, the predicted quintet-suppression factor, is depicted in Fig. 2.5 and shows the trend with energy of all modern investigations and only weak quintet-state suppression of the $D + D$ neutrons at the relevant low energies. Other predictions or data parameterizations show also weak or no suppression except for the higher laboratory energy range above ≈ 100 keV.

The five-nucleon systems which have been thoroughly investigated experimentally have so far not been treated theoretically by truly microscopic methods. The calculations were either in the framework of resonating-group methods (RGM) or in R-matrix parametrization of experimental data at higher energies, i.e. above the astrophysically interesting energies but encompassing the $J = 3/2^+$ resonance region. Recently ab initio many-body calculations using again the nucleon–nucleon interaction but also three-body forces as input have had stunning successes in describing low-lying states of a number of light nuclei [40, 41], e.g. for $^{10,11}\text{B}$ and $^{12,13}\text{C}$.

Two successful methods are the *Green's function Monte Carlo* (GFMC) and the *no-core shell model* (NCSM) methods. Recently, these have been applied to nuclear (astrophysically relevant) reactions such as ${}^3\text{H}(\alpha, \gamma){}^7\text{Li}$, ${}^3\text{He}(\alpha, \gamma){}^7\text{Be}$, and ${}^7\text{Be}(p, \gamma){}^8\text{Be}$ [42]. Now a recent letter [43, 44] presented the first ab initio many-body calculation of the ${}^3\text{H}(\text{d}, \text{n}){}^4\text{He}$ and ${}^3\text{He}(\text{d}, \text{p}){}^4\text{He}$ fusion reactions in the framework of the ab initio NCSM/RGM approach, see e.g. [45] and references therein, in an effort to unify the description of the (bound-state) nuclei involved and the (scattering-state) reaction mechanism, starting from the chiral N^3LO NN interaction. S -factors in the energy range from almost zero to 2 MeV across the resonance region were calculated and—in view of the approximations used, e.g. the $NNLO$ force—show quite satisfactory agreement with the data, especially in the resonance regions, but for the ${}^3\text{He}(\text{d}, \text{p}){}^4\text{He}$ reaction the data in the resonance region have larger discrepancies than for the ${}^3\text{H}(\text{d}, \text{n}){}^4\text{He}$ reaction. In the future much better agreement can be expected. For details including the wealth of all available data and their comparison with the calculations the reader is referred to the original articles.

2.5.2 Effect of Electron Screening

In Fig. 2.6 the effect of electronic screening is clearly visible for the reaction ${}^3\text{He}(\text{d}, \text{p}){}^4\text{He}$, but not so evident for ${}^3\text{H}(\text{d}, \text{n}){}^4\text{He}$. Of course, purely nuclear calculations do not describe this part of the S -factor, and a consistent theory of the screening is still missing. Precise extrapolations of the nuclear S -factor together with precise measurements of the cross-sections which are difficult due to the low energies could help to pin down the screening details, maybe also including possible polarization effects on the screening. The cross-section enhancement could be potentially useful for fusion-energy applications although the energy range of the enhancement is below that where fusion reaction yields have their maxima.

2.6 New Aspects of Polarized Fusion

The developments in fusion-energy experiments (tokamaks, laser fusion, stellarators, and linear fusion devices) and at the same time the increasing certainty of the interrelations between fossil fuel consumption, climate changes, population dynamics and energy needs make it necessary to convince the fusion-energy community of the importance of “polarized fusion”. Therefore, increased efforts and new developments in this field are mandatory. A few items will be touched upon here.

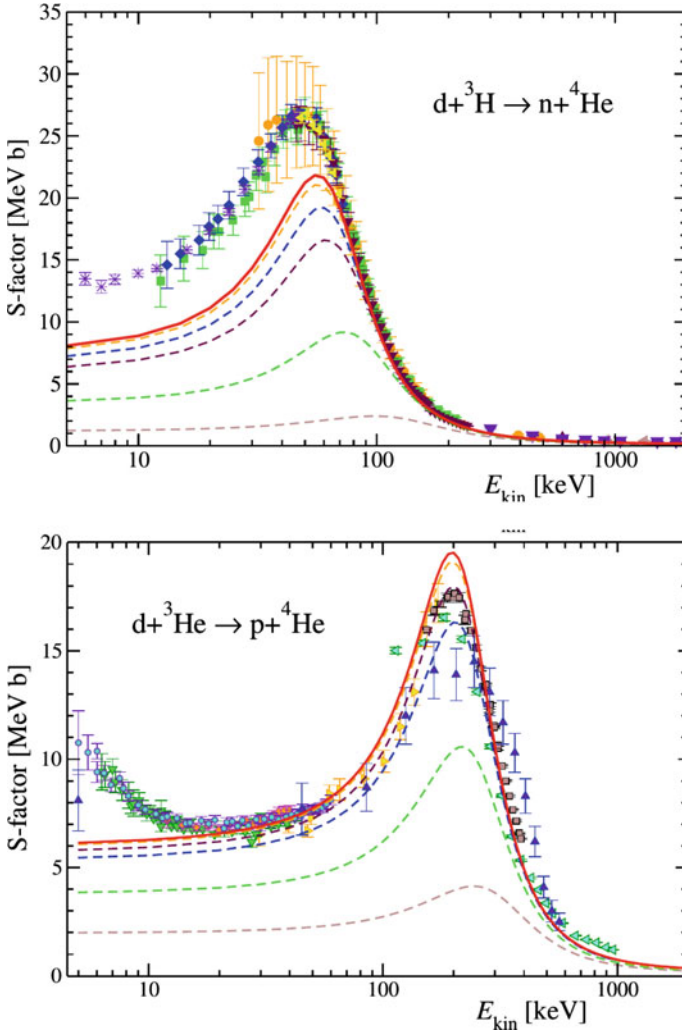


Fig. 2.6 S -factors of the $D + T$ and $D + {}^3\text{He}$ reactions. Shown are the sets of all available data together with different ab initio calculations (for details see [44]). In the lower figure the effect of screening is clearly visible at low energy where an approximately constant S -factor would be expected without screening. Figures adapted from [44] with permission of the author P. Navratil. Copyrighted by the American Physical Society

2.6.1 Rate Enhancement and Electron Screening

From relatively simple considerations the conclusion was drawn that for the five-nucleon particle reactions ${}^3\text{H}(d, n){}^4\text{He}$ and ${}^3\text{He}(d, p){}^4\text{He}$ an enhancement of the fusion cross-sections and reaction rates of up to a factor $f = 1.5$ (for the case of a pure

transition through the $J = 3/2^+$ resonance state can be expected when both incident reaction partners are fully spin-polarized. Below the resonance energy the amount of enhancement is not so clear because other partial-wave states may have a stronger influence on the cross-sections, relative to the dominant $3/2^+$ state. In addition, electron screening modifies the cross-section, and the effect of the polarization on this modification/enhancement is unclear and should be measured. Figure 2.6 shows the experimental low-energy behaviour of the two five-nucleon reactions. For the $D + D$ reactions strong screening has also been measured, see [46].

2.6.2 *Pellet Implosion Dynamics*

In the case of inertial fusion using the compression of a fuel pellet by laser or ion beams seems to follow a dynamics which can additionally increase the gain by polarizing the fuel by an additional factor. According to recent references [47] numerical simulations show that, depending on the value of f and on a number of special conditions of pellet design etc., an additional enhancement factor seems to arise which—in the case discussed—changed the situation from “no ignition” to “ignition”. Conversely, it is shown that the ignition conditions (temperature and density) can be somewhat relaxed when using polarized fuel. Further studies of this effect are important and necessary.

2.6.3 *Technical Questions*

The provision of either solid or liquid highly polarized pellets for inertial fusion may be easier to achieve than very intense polarized beams to be injected in magnetic-fusion devices. The hopes expressed in [48] of having “amperes of polarized nuclei at acceptable power cost” have not been borne out. Perhaps polarized molecules could be produced in large quantities [49]. These ideas, however, need thorough and expensive investigations in the future. A recent proposal by [50] is to separate brute-force polarized hydrogen molecules in the ortho spin-state with total spin $I = 1$ by a strong superconducting Stern–Gerlach magnet with the expectation to obtain beam intensities (or densities) higher by an order of magnitude as compared to the atomic-beam intensities from ABS which seem to have reached some saturation. At the proposed temperature of the molecules of $T = 20\text{ K}$ about 99.8% of the molecules are in the para state (the para state has $I = 0$) and the ortho molecules have to be “filtered” out from this background. Because the magnetic interaction is with the nuclear magnetic moment only, the deflection is very small, see [51]. The polarization will depend on the degree of selectivity of one of the nine hyperfine states against different background. For the measurement of the polarization of the molecules the Lambshift polarimeter developed recently is an ideal instrument, see [52, 53].

2.6.4 Preservation of Polarization on Injection

The preservation of the fuel polarization either during the transport of the polarized particles to the reactor, during injection and in the plasma collisions has been discussed already quite early. Kulsrud [1] concluded from quite general considerations that depolarization would not be a problem in magnetic-confinement fusion, and More [54] came to similar conclusions for the case of inertial confinement. The authors of [7, 8] recently proposed an experiment to investigate this question in a polarized HD molecular target where the idea of observing the γ 's from the reaction ${}^2\text{H} + {}^1\text{H} \rightarrow {}^3\text{He} + \gamma$ was discarded in favor of the D + D reaction neutrons because of their much higher cross-section.

2.7 Summary and Conclusions

Due to the slow, but visible progress in the physics and technologies of fusion energy, it is appropriate to focus again on the old ideas of using polarized fuel in MCF as well as ICF devices and the advantages this could offer. For the five-nucleon reactions we have quantitative results at hand, but for the D + D reactions the complicated reaction mechanism requires renewed and increased theoretical and experimental efforts to decide on reaction-rate suppression or enhancement, or effects on emission directions. The questions of production of high-density highly polarized beams and targets, of polarization preservation on injection and ignition, and others are largely unanswered and open interesting fields of research in the future.

Acknowledgments The author thanks Ralf Engels for many fruitful discussions and ideas.

Appendix

The cross-sections for the two cases spin-1 on spin-1/2 and spin-1 on spin-1 consist of the unpolarized cross-sections, a number of vector and tensor analyzing powers and spin-correlation coefficients. The coordinate system chosen is with the z axis in the incident momentum direction, the y axis in the direction of the normal to the scattering plane and the x axis forming a righthanded system with both. The Cartesian representation is chosen.

All "polarized" cross-sections are ϕ dependent and this dependence must be worked out for the contribution from each observable (for the determination of this "azimuthal complexity" see [4]) and is not given here.

All observables compatible with parity conservation and hermiticity are listed. For the special spin-1 on spin-1 case of deuterons on deuterons a number of terms are redundant due to the identity of the entrance-channel particles.

Spin-1 Beam on Spin-1/2 Target

$$\begin{aligned}
 \left(\frac{d\sigma(\Theta, \phi)}{d\Omega} \right)_{\Phi=0} &= \left(\frac{d\sigma(\Theta)}{d\Omega} \right)_0 \left\{ 1 + \frac{3}{2} A_y^{(b)}(\Theta) p_y + A_y^{(t)} q_y + \frac{1}{2} A_{zz}^{(b)}(\Theta) p_{zz} + \frac{2}{3} A_{xz}^{(b)}(\Theta) p_{xz} \right. \\
 &\quad + \frac{1}{6} A_{xx-yy}^{(b)}(\Theta) p_{xx-yy} \\
 &\quad + \frac{3}{2} [C_{x,x}(\Theta) p_x q_x + C_{y,y}(\Theta) p_y q_y + C_{z,z}(\Theta) p_z q_z \\
 &\quad \quad + C_{z,x}(\Theta) p_z q_x + C_{x,z}(\Theta) p_x q_z] \\
 &\quad + \frac{2}{3} [C_{xy,x}(\Theta) p_{xy} q_x + C_{yz,x}(\Theta) p_{yz} q_x \\
 &\quad \quad + C_{xz,y}(\Theta) p_{xz} q_y + C_{xy,z}(\Theta) p_{xy} q_z + C_{yz,z}(\Theta) p_{yz} q_z] \\
 &\quad \left. + \frac{1}{6} C_{xx-yy,y}(\Theta) p_{xx-yy} q_y + \frac{1}{2} C_{zz,y}(\Theta) p_{zz} q_y \right\}. \quad (2.14)
 \end{aligned}$$

The symbols b , t , p , and q designate the beam, the target, and the beam and target polarizations, respectively. Here 18 observables are measurable: one unpolarized cross-section, two vector and three tensor analyzing powers, and 12 correlation coefficients.

General Spin-1 on Spin-1 Case

$$\begin{aligned}
 \left(\frac{d\sigma(\Theta, \phi)}{d\Omega} \right)_{\Phi=0} &= \left(\frac{d\sigma(\Theta)}{d\Omega} \right)_0 \left\{ 1 + \frac{3}{2} [A_y^{(b)}(\Theta) p_y + A_y^{(t)} q_y] + \frac{1}{2} [A_{zz}^{(b)}(\Theta) p_{zz} + A_{zz}^{(t)}(\Theta) q_{zz}] \right. \\
 &\quad + \frac{1}{6} [A_{xx-yy}^{(b)}(\Theta) p_{xx-yy} + A_{xx-yy}^{(t)}(\Theta) q_{xx-yy}] \\
 &\quad + \frac{2}{3} [A_{xz}^{(b)}(\Theta) p_{xz} + A_{xz}^{(t)}(\Theta) q_{xz}] \\
 &\quad + \frac{9}{4} [C_{y,y}(\Theta) p_y q_y + C_{x,x}(\Theta) p_x q_x + C_{x,z}(\Theta) p_x q_z \\
 &\quad \quad + C_{z,x}(\Theta) p_z q_x + C_{z,z}(\Theta) p_z q_z] \\
 &\quad + \frac{3}{4} [C_{y,zz}(\Theta) p_y q_{zz} + C_{zz,y}(\Theta) p_{zz} q_y] \\
 &\quad + C_{y,xz}(\Theta) p_y q_{xz} + C_{xz,y}(\Theta) p_{xz} q_y + C_{x,yz}(\Theta) p_x q_{yz} \\
 &\quad + C_{yz,x}(\Theta) p_{yz} q_x + C_{z,yz}(\Theta) p_z q_{yz} + C_{yz,z}(\Theta) p_{yz} q_z \\
 &\quad + \frac{1}{4} [C_{y,xx-yy}(\Theta) p_y q_{xx-yy} + C_{xx-yy,y}(\Theta) p_{xx-yy} q_y \\
 &\quad \quad + C_{zz,zz}(\Theta) p_{zz} q_{zz}] \\
 &\quad \left. + \frac{1}{3} [C_{zz,xz}(\Theta) p_{zz} q_{xz} + C_{xz,zz}(\Theta) p_{xz} q_{zz}] \right\}
 \end{aligned}$$

$$\begin{aligned}
& + \frac{1}{12} [C_{zz,xx-yy}(\Theta)p_{zz}q_{xx-yy} + C_{xx-yy,zz}(\Theta)p_{xx-yy}q_{zz}] \\
& + \frac{4}{9} [C_{xz,xz}(\Theta)p_{xz}q_{xz} + C_{yz,yz}(\Theta)p_{yz}q_{yz}] \\
& + \frac{8}{9} [C_{xy,yz}(\Theta)p_{xy}q_{yz} + C_{yz,xy}(\Theta)p_{yz}q_{xy}] \\
& + \frac{16}{9} C_{xy,xy}(\Theta)p_{xy}q_{xy} \\
& + \frac{1}{9} [C_{xz,xx-yy}(\Theta)p_{xz}q_{xx-yy} + C_{xx-yy,xz}(\Theta)p_{xx-yy}q_{xz}] \\
& + \frac{1}{36} C_{xx-yy,xx-yy}(\Theta)p_{xx-yy}q_{xx-yy} \\
& + \frac{1}{2} [C_{x,xy}(\Theta)p_xq_{xy} + C_{xy,x}(\Theta)p_{xy}q_x + C_{z,xy}(\Theta)p_zq_{xy} \\
& \quad + C_{xy,z}(\Theta)p_{xy}q_z] \}. \tag{2.15}
\end{aligned}$$

Here the number of observables (in parentheses for $D + D$) is 41 (24): one unpolarized cross-section, two (one) vector and six (three) tensor analyzing powers, and 32 (19) correlation coefficients.

References

1. R.M. Kulsrud, H.P. Furth, E.J. Valeo, M. Goldhaber, Phys. Rev. Lett. **49**, 1248 (1982)
2. R.M. Kulsrud, Nucl. Instr. Meth. **A271**, 4 (1988)
3. M. Tanaka (ed), Proceedings of the RCNP Workshop on Spin Polarized Nucl. Fusions (POLUSION99), RCNP Osaka (1999)
4. H. Paetz gen. Schieck, Eur. Phys. J. A **44**, 321 (2010)
5. H. Paetz gen. Schieck, *Nuclear Physics with Polarized Particles*, Lecture Notes in Physics, vol. 842 (Springer, Heidelberg, 2012)
6. A. Honig, A. Sandorfi, in *Proceedings 17th International AIP Conference on Spin Physics Symposium (SPIN2006)*, ed. by K. Imai, T. Murakami, N. Saito, K. Tanida, vol. 915, Kyoto (2007) p. 1010
7. J.-P. Didelez, C. Deutsch, J. Phys. Conf. Series **295**, 012169 (2011)
8. J.-P. Didelez, C. Deutsch, Laser Part. Beams **29**, 169 (2011)
9. A. Deltuva, A. Fonseca, Phys. Rev. C **76**, 021001(R) (2007)
10. A. Deltuva, A. Fonseca, Phys. Rev. C **81**, 054002 (2010)
11. A. Huke, K. Czerski, P. Heide, G. Ruprecht, N. Targosz, W. Żebrowski. Phys. Rev. C **78**, 015803 (2008)
12. C. Rolfs, E. Somorjai, Nucl. Instr. Meth. Phys. Res. **B 99**, 297 (1995)
13. Ch. Leemann, H. Bürgisser, P. Huber, U. Rohrer, H. Paetz gen. Schieck, F. Seiler. Helv. Phys. Acta **44**, 141 (1971)
14. Ch. Leemann, H. Bürgisser, P. Huber, U. Rohrer, H. Paetz gen. Schieck, F. Seiler, Ann. Phys. (N.Y.) **66**, 810 (1971)
15. W.H. Geist, C.R. Brune, H.J. Karwowski, E.J. Ludwig, K.D. Veal, G.M. Hale, Phys. Rev. C **60**, 054003 (1999)
16. D. Braizinha, C.R. Brune, A.M. Eiró, B.M. Fisher, H.J. Karwowski, D.S. Leonard, E.J. Ludwig, F.D. Santos, I.J. Thompson, Phys. Rev. C **69**, 0246008 (2004)
17. H. Grunder, R. Gleyvod, G. Lietz, G. Morgan, H. Rudin, F. Seiler, A. Stricker, Helv. Phys. Acta **44**, 662 (1971)

18. F. Seiler, E. Baumgartner, Nucl. Phys. A **153**, 193 (1970)
19. G. Hale, G. Doolen, LA-9971-MS, Los Alamos (1984)
20. R.J. Knize, in *Proceedings of the 6th International Symposium on Polarization Phenomena in Nuclear Physics* ed. by M. Kondo et al., Osaka (1985). Suppl. J. Phys. Soc. Jpn. **55** (1986)
21. H.M. Hofmann, in *Proceedings of the Models and Methods in Few-Body Physics*, Lisboa, Portugal, 1986, eds. by L.S. Ferreira, A.C. Fonseca, L. Streit, Lecture Notes in Physics, vol. 273 (Springer, Berlin, 1987) p. 243
22. S. Lemaître, H. Paetz gen. Schieck. Few-Body Syst. **9**, 155 (1990)
23. S. Lemaître, H. Paetz gen. Schieck, Ann. Phys. (Leipzig) **2**, 503 (1993)
24. O. Geiger, S. Lemaître, H. Paetz gen. Schieck. Nucl. Phys. A**586**, 140 (1995)
25. A. Lane, R. Thomas, Rev. Mod. Phys. **30**, 257 (1958)
26. D. Fick, U. Weiß, Z. Phys. **265**, 87 (1973)
27. P. Kozma, P. Bém, Nucl. Phys. A **442**, 17 (1985)
28. D.S. Leonard, H.J. Karwowski, C.R. Brune, B. Fisher, E.J. Ludwig, Phys. Rev. C **73**, 045801 (2006)
29. T. Katabuchi, K. Kudo, K. Masuno, T. Iizuka, Y. Aoki, Y. Tagishi, Phys. Rev. C **64**, 047601 (2001)
30. A. Imig, C. Düweke, R. Emmerich, J. Ley, K.O. Zell, H. Paetz gen. Schieck. Phys. Rev. C **73**, 024001 (2006)
31. K.A. Fletcher, Z. Ayer, T.C. Black, R.K. Das, H.J. Karwowski, E.J. Ludwig, G.M. Hale, Phys. Rev. C **49**, 2305 (1994)
32. J.S. Zhang, K.F. Liu, G.W. Shuy, Phys. Rev. Lett. **55**, 1649 (1985)
33. J.S. Zhang, K.F. Liu, G.W. Shuy, Phys. Rev. Lett. **57**, 1410 (1986)
34. D. Fick, H.M. Hofmann, Phys. Rev. Lett. **55**, 1650 (1983)
35. H.M. Hofmann, D. Fick, Phys. Rev. Lett. **52**, 2038 (1984)
36. H.M. Hofmann, D. Fick, Phys. Rev. Lett. **57**, 1410 (1986)
37. E. Uzu, S. Oryu, M. Tanifuji, in [3], p. 30
38. E. Uzu (2002), [arXiv:nucl-th/0210026](https://arxiv.org/abs/nucl-th/0210026)
39. J.S. Zhang, K.F. Liu, G.W. Shuy, Phys. Rev. C **60**, 054614 (1999)
40. C. Pieper, V.R. Pandharipande, R.B. Wiringa, J. Carlson, Phys. Rev. C **64**, 014001 (2001)
41. E. Epelbaum, H.-W. Hammer, U.-G. Meißner, Rev. Mod. Phys. **81**, 1773 (2009)
42. P. Navrátil, S. Quaglioni, I. Stetcu, B.R. Barrett, J. Phys. G **36**, 083101 (2009)
43. P. Navrátil, S. Quaglioni (2011), [arXiv:1110.0460v1](https://arxiv.org/abs/1110.0460v1) [nucl-th]
44. P. Navrátil, S. Quaglioni, Phys. Rev. Lett. **108**, 042503 (2012)
45. P. Navrátil, S. Quaglioni, Phys. Rev. C **83**, 044609 (2011)
46. F. Raiola et al., Eur. Phys. J. A **13**, 377 (2002)
47. M. Temporal, V. Brandon, B. Canaud, J.P. Didelez, R. Fedosejevs, R. Ramis, Nucl. Fusion **52**, 103011 (2012)
48. Physics Today, AIP New York, 8/(1982)
49. R. Engels et al., Phys. Rev. Lett. **115**, 113007 (2015)
50. D.M. Nikolenko, I.A. Rachek, Yu.V. Shestakov, D.K. Toporkov, in *Proceedings of the XIVth International Workshop on Polarized Sources, Targets, and Polarimeters*, St. Petersburg (2011)
51. R. Frisch, O. Stern, Z. Phys. **85**, 4 (1933)
52. R. Engels, R. Emmerich, J. Ley, G. Tenckhoff, H. Paetz gen. Schieck, Rev. Sci. Instr. **74**, 345 (2003)
53. R. Engels, R. Kröll, N. Nikolaev, F. Rathmann, H. Ströher, N. Chernov, L. Kochenda, P. Kravtsov, V. Trofimov, A. Vasiliev, K. Grigoriev, M. Mikirtychiants, S. Kiselev, M. Marusina, H. Paetz gen. Schieck, Fusion of polarized deuterons, in *Proceedings of the HIF2010 Conference* (GSI, Darmstadt, 2010)
54. R.M. More, Phys. Rev. Lett **51**, 396 (1983)



<http://www.springer.com/978-3-319-39470-1>

Nuclear Fusion with Polarized Fuel

Ciullo, G.; Engels, R.; Büscher, M.; Vasilyev, A. (Eds.)

2016, XIV, 154 p. 48 illus., 14 illus. in color., Hardcover

ISBN: 978-3-319-39470-1